

Supporting Information

5

Thiacalix[4]arene-protected alkynyl Ag_n (n =9, 18) nanoclusters: Syntheses, structural characterizations, photocurrent responses and fluorescence properties

10

Wen-Xuan Xie,[‡] Chun-Hui Xue,[‡] Meng Liu, Kun Zhou,^{*a} Hui-Hao Gu, Jiu-Yu Ji, Bao-Kuan Chen,^{*a}
Na Liu, Yan-Feng Bi^{*a}

School of Petrochemical Engineering, School of Artificial Intelligence and Software, Liaoning Petrochemical University, Fushun 113001, China. Tel/Fax: (+86) -24-56861709; E-mail: zhouk800@nenu.edu.cn, chenbaokuan@lnpu.edu.cn, biyanfeng@lnpu.edu.cn

15

20

X-ray crystallography

Crystal data and structure refinements for **Ag₉** and **Ag₁₈** are listed in Table S1. Selected bond lengths, Ag···Ag interactions (Å) data and bond angles for **Ag₉** are listed in Table S2-Table S4. Selected bond lengths, Ag···Ag interactions (Å) data and bond angles for **Ag₁₈** are listed in Table S5-Table S7. Comparison of the average Ag···Ag interactions (Å) and the average bond distances (Å) of important bonds in **Ag₉** and **Ag₁₈** are listed in Table S8 and Table S9, respectively.

Table S1. Crystal data, data collection and structure refinement details for Ag₉ and Ag₁₈

	Ag₉	Ag₁₈
Formula	C ₁₃₄ H ₁₈₀ Ag ₁₈ F ₆ Na ₄ O ₂₅ S ₈ Sb	C ₁₃₆ H ₁₇₆ Ag ₁₈ F ₆ O ₁₆ S ₈
Formula weight	4716.62	4378.90
Crystal system	Orthorhombic	Monoclinic
Space group	I mmm	C 2/m
<i>a</i> (Å)	15.2729(8)	22.163(2)
<i>b</i> (Å)	15.4945(8)	21.603(2)
<i>c</i> (Å)	39.339(2)	19.2809(18)
<i>α</i> (Å)	90	90
<i>β</i> (Å)	90	119.703(3)
<i>γ</i> (Å)	90	90
V (Å ³)	9309.4(8)	8018.5(14)
Z	2	2
Dc/g cm ⁻³	1.683	1.814
μ/mm ⁻¹	2.144	2.306
F(000)	4614	4296
Reflection collected	15445	28325
Unique reflections	4495	7220
Parameters	318	641
R _{int}	0.0331	0.0841
GOF	1.111	1.046
R ₁ ^a [I>2σ(I)]	0.0687	0.0550
wR ₂ ^b (all data)	0.1849	0.1499

$${}^a R_1 = \Sigma ||F_o| - |F_c|| / \Sigma |F_o|; {}^b wR_2 = \{ \Sigma [w(F_o^2 - F_c^2)^2] / \Sigma [w(F_o^2)^2] \}^{1/2}$$

Table S2. Selected bond distances (Å) data for Ag₉

Bond	Bond length	Bond	Bond length
Ag(1)-C(15)	2.243(10)	Ag(2)-O(2)#1	2.395(9)
Ag(1)-O(2)	2.433(4)	Ag(2)-O(2)	2.395(9)
Ag(1)-O(1)	2.441(4)	Ag(3)-C(15)	2.129(11)
Ag(1)-S(1)	2.484(2)	Ag(3)-C(15)#2	2.129(11)
Ag(1)-C(16)	2.486(9)	Ag(3)-O(3)	2.41(3)
Ag(2)-O(1)#1	2.342(10)	Ag(4)-C(15)	2.171(13)
Ag(2)-O(1)	2.342(10)	Ag(4)-C(15)#3	2.171(13)

Symmetry transformations used to generate equivalent atoms: #1 -x,-y,z, #2 x,-y,z, #3 -x,y,z.

5

Table S3. Ag \cdots Ag interactions (Å) data for Ag₉

Metal \cdots metal contact	Distance	Metal \cdots metal contact	Distance
Ag(1)-Ag(3)	3.1848(12)	Ag(3)-Ag(4)	2.8341(15)
Ag(1)-Ag(4)	3.2188(13)	Ag(3)-Ag(4)#1	2.8341(15)
Ag(1)-Ag(2)	3.2591(10)	Ag(4)-Ag(4)#1	3.331(3)

Symmetry transformations used to generate equivalent atoms: #1 -x,-y,z.

Table S4. Selected bond angle (°) data for Ag₉

Bond	Bond angle	Bond	Bond angle
C(15)-Ag(1)-O(2)	116.3(4)	O(1)#1-Ag(2)-O(1)	178.9(4)
C(15)-Ag(1)-O(1)	115.0(3)	O(1)#1-Ag(2)-O(2)#1	90.000(3)
O(2)-Ag(1)-O(1)	86.8(3)	O(1)-Ag(2)-O(2)#1	90.000(2)
C(15)-Ag(1)-S(1)	160.6(3)	O(1)#1-Ag(2)-O(2)	90.000(2)
O(2)-Ag(1)-S(1)	77.37(18)	O(1)-Ag(2)-O(2)	90.000(2)
O(1)-Ag(1)-S(1)	77.89(18)	O(2)#1-Ag(2)-O(2)	180.0(4)
C(15)-Ag(1)-C(16)	28.7(4)	C(15)-Ag(3)-C(15)#2	169.8(7)
O(2)-Ag(1)-C(16)	120.4(3)	C(15)-Ag(3)-O(3)	94.5(4)
O(1)-Ag(1)-C(16)	139.9(3)	C(15)#2-Ag(3)-O(3)	94.5(4)
S(1)-Ag(1)-C(16)	133.1(3)	C(15)-Ag(4)-C(15)#3	155.3(6)

Symmetry transformations used to generate equivalent atoms: #1 -x,-y,z, #2 x,-y,z, #3 -x,y,z.

10

Table S5. Selected bond distances (Å) data for Ag₁₈

Bond	Bond length	Bond	Bond length
Ag(1)-C(21)	2.224(12)	Ag(4)-O(2)	2.400(6)
Ag(1)-O(1)#1	2.447(5)	Ag(4)-C(28)	2.45(3)
Ag(1)-O(1)	2.447(5)	Ag(4)-O(1)#1	2.454(6)
Ag(1)-S(1)	2.501(3)	Ag(4)-S(2)	2.514(2)
Ag(1)-C(22)	2.508(18)	Ag(5)-C(27)	1.91(5)
Ag(1)-C(22)#1	2.508(18)	Ag(5)-C(33)	2.297(12)
Ag(2)-O(1)#1	2.367(6)	Ag(5)-C(34)#1	2.71(2)
Ag(2)-O(1)	2.367(6)	Ag(6)-C(27)	1.89(4)
Ag(2)-O(2)#1	2.415(6)	Ag(6)-C(21)	2.048(12)
Ag(2)-O(2)	2.415(6)	C(21)-Ag(6A)#1	2.345(11)
Ag(3)-C(33)	2.294(12)	C(21)-Ag(6A)	2.345(11)
Ag(3)-C(34)#1	2.330(18)	C(33)-Ag(5A)#1	2.059(10)
Ag(3)-C(34)	2.330(18)	C(33)-Ag(5A)	2.059(10)
Ag(3)-O(2)	2.397(6)	C(33)-Ag(6A)#3	2.566(11)
Ag(3)-O(2)#1	2.397(6)	C(33)-Ag(6A)#2	2.566(11)
Ag(3)-S(3)	2.506(3)	O(3)-Ag(6A)	2.33(2)
Ag(4)-C(27A)	2.24(3)	O(4)-Ag(5A)#2	2.361(17)
Ag(4)-C(27)	2.33(4)	C(27A)-Ag(5A)	2.22(3)
Ag(4)-C(28A)	2.36(3)	C(27A)-Ag(6A)	2.52(2)

Symmetry transformations used to generate equivalent atoms: #1 x,-y+1,z, #2 -x+1,y,-z+1, #3 -x+1,-y+1,-z+1.

Table S6. Ag...Ag interactions (Å) data for Ag₁₈

Metal...metal contact	Distance	Metal...metal contact	Distance
Ag(1)-Ag(6)#1	3.1187(17)	Ag(4)-Ag(5)	3.222(5)
Ag(1)-Ag(6)	3.1187(17)	Ag(4)-Ag(5A)	3.323(4)
Ag(1)-Ag(2)	3.2534(14)	Ag(5)-Ag(6)	2.441(3)
Ag(2)-Ag(3)	3.2266(15)	Ag(5)-Ag(5)#1	2.758(10)
Ag(2)-Ag(4)	3.2784(9)	Ag(5)-Ag(5)#2	2.938(9)
Ag(2)-Ag(4)#1	3.2785(9)	Ag(6)-Ag(6)#1	2.286(3)
Ag(3)-Ag(5A)#1	3.043(4)	Ag(5A)-Ag(6A)#2	2.932(4)
Ag(3)-Ag(5A)	3.043(4)	Ag(5A)-Ag(5A)#1	3.103(9)
Ag(3)-Ag(5)#1	3.219(4)	Ag(5A)-Ag(5A)#2	3.209(8)
Ag(3)-Ag(5)	3.219(4)	Ag(6A)-Ag(6A)#1	2.823(4)
Ag(4)-Ag(6)	3.1013(16)		

Symmetry transformations used to generate equivalent atoms: #1 x,-y+1,z, #2 -x+1,y,-z+1.

Table S7. Selected bond angle (°) data for Ag₁₈

Bond	Bond angle	Bond	Bond angle
C(21)-Ag(1)-O(1)#1	113.2(3)	C(33)-Ag(3)-S(3)	151.2(4)
C(21)-Ag(1)-O(1)	113.2(3)	C(34)#1-Ag(3)-S(3)	124.5(5)
O(1)#1-Ag(1)-O(1)	87.2(3)	C(34)-Ag(3)-S(3)	124.5(5)
C(21)-Ag(1)-S(1)	164.7(4)	O(2)-Ag(3)-S(3)	78.40(14)
O(1)#1-Ag(1)-S(1)	77.31(13)	O(2)#1-Ag(3)-S(3)	78.40(14)
O(1)-Ag(1)-S(1)	77.31(14)	C(27A)-Ag(4)-C(28A)	29.8(10)
C(21)-Ag(1)-C(22)	29.6(5)	C(27A)-Ag(4)-O(2)	113.8(8)
O(1)#1-Ag(1)-C(22)	138.5(5)	C(27)-Ag(4)-O(2)	112.3(12)
O(1)-Ag(1)-C(22)	119.5(5)	C(28A)-Ag(4)-O(2)	141.9(7)
S(1)-Ag(1)-C(22)	135.9(5)	C(27)-Ag(4)-C(28)	33.5(12)
C(21)-Ag(1)-C(22)#1	29.6(5)	O(2)-Ag(4)-C(28)	132.1(7)
O(1)#1-Ag(1)-C(22)#1	119.5(5)	C(27)-Ag(4)-O(1)#1	109.9(11)
O(1)-Ag(1)-C(22)#1	138.5(5)	O(2)-Ag(4)-O(1)#1	87.9(2)
S(1)-Ag(1)-C(22)#1	135.9(5)	C(28)-Ag(4)-O(1)#1	128.2(7)
C(22)-Ag(1)-C(22)#1	21.4(10)	C(27A)-Ag(4)-S(2)	161.7(6)
O(1)#1-Ag(2)-O(1)	91.0(3)	C(27)-Ag(4)-S(2)	167.4(11)
O(1)#1-Ag(2)-O(2)#1	175.71(19)	C(28A)-Ag(4)-S(2)	134.4(8)
O(1)-Ag(2)-O(2)#1	89.61(19)	O(2)-Ag(4)-S(2)	77.97(14)
O(1)#1-Ag(2)-O(2)	89.61(19)	C(28)-Ag(4)-S(2)	134.1(7)
O(1)-Ag(2)-O(2)	175.71(19)	O(1)#1-Ag(4)-S(2)	76.70(13)
O(2)#1-Ag(2)-O(2)	89.5(3)	C(27)-Ag(5)-C(33)	170.4(14)
C(33)-Ag(3)-C(34)#1	32.9(5)	C(27)-Ag(5)-C(34)#1	142.2(14)
C(33)-Ag(3)-C(34)	32.9(5)	C(33)-Ag(5)-C(34)#1	28.8(5)
C(34)#1-Ag(3)-C(34)	48.7(11)	C(27)-Ag(6)-C(21)	156.9(15)
C(33)-Ag(3)-O(2)	120.1(2)	C(33)-Ag(5A)-C(27A)	169.0(7)
C(34)#1-Ag(3)-O(2)	107.7(6)	C(33)-Ag(5A)-O(4)#2	95.9(5)
C(34)-Ag(3)-O(2)	152.7(5)	O(3)-Ag(6A)-C(21)	112.0(7)
C(33)-Ag(3)-O(2)#1	120.1(2)	O(3)-Ag(6A)-C(27A)	113.1(10)
C(34)#1-Ag(3)-O(2)#1	152.7(5)	C(21)-Ag(6A)-C(27A)	115.9(6)
C(34)-Ag(3)-O(2)#1	107.7(6)	C(21)-Ag(6A)-C(33)#3	106.6(3)
O(2)-Ag(3)-O(2)#1	90.4(3)		

Symmetry transformations used to generate equivalent atoms: #1 x,-y+1,z, #2 -x+1,y,-z+1, #3 -x+1,-y+1,-z+1.

Table S8. Comparison of the average Ag \cdots Ag interactions (Å) in Ag₉ and Ag₁₈

	Ag ₅ @TC4A	Ag ₄ @('BuC \equiv C) ₄	Between Ag ₅ @TC4A and Ag ₄ @('BuC \equiv C) ₄	Between Ag ₉ and Ag ₉
Ag ₉	3.259 Å	3.000 Å	3.202 Å	6.500 Å
Ag ₁₈	3.259 Å	2.648 Å	3.156 Å	3.083 Å

5 Table S9. Comparison of the average bond distances (Å) of important bonds in Ag₉ and Ag₁₈

	The Ag-S bond in Ag ₅ @TC4A	The Ag-O bond in Ag ₅ @TC4A	The Ag-C bond in Ag ₄ @('BuC \equiv C) ₄	The Ag-O bond attached to CH ₃ OH/CF ₃ COO ⁻
Ag ₉	2.484 Å	2.391 Å	2.222 Å	2.410 Å (CH ₃ OH)
Ag ₁₈	2.507 Å	2.411 Å	2.309 Å	2.346 Å (CF ₃ COO ⁻)

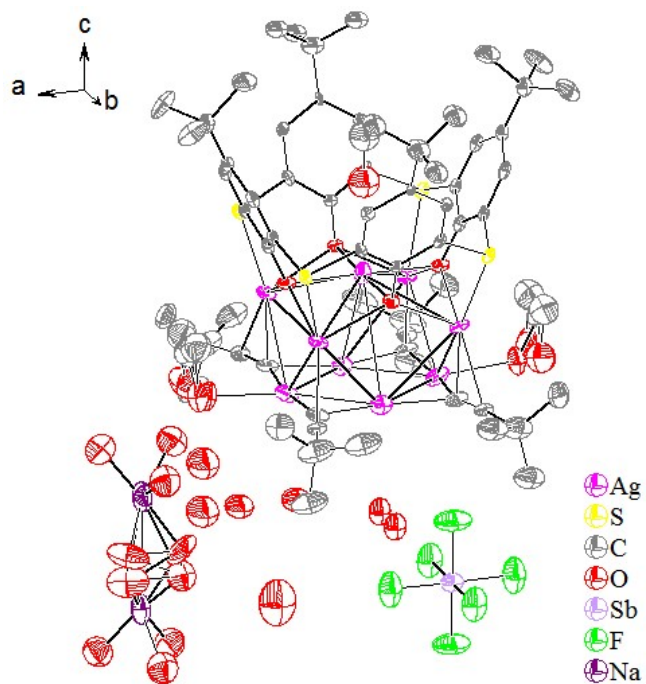


Fig. S1 30% Ellipsoid representations of Ag_9 containing all disordered atoms. All the hydrogen atoms have been omitted.

As shown in Fig. S2, although Sb1 is still highly over-assigned, both of the charge conservation and the rationality of crystal data refinement have been taken into consideration, the assignment of atom Sb1 is reasonable.

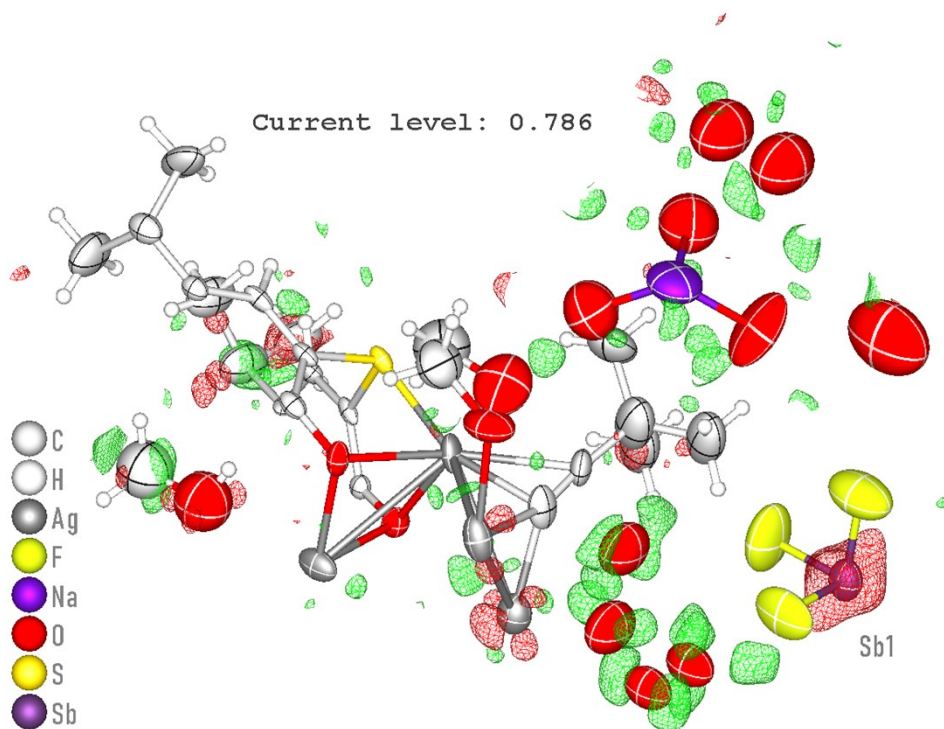


Fig. S2 The residual density plot of Ag_9 .

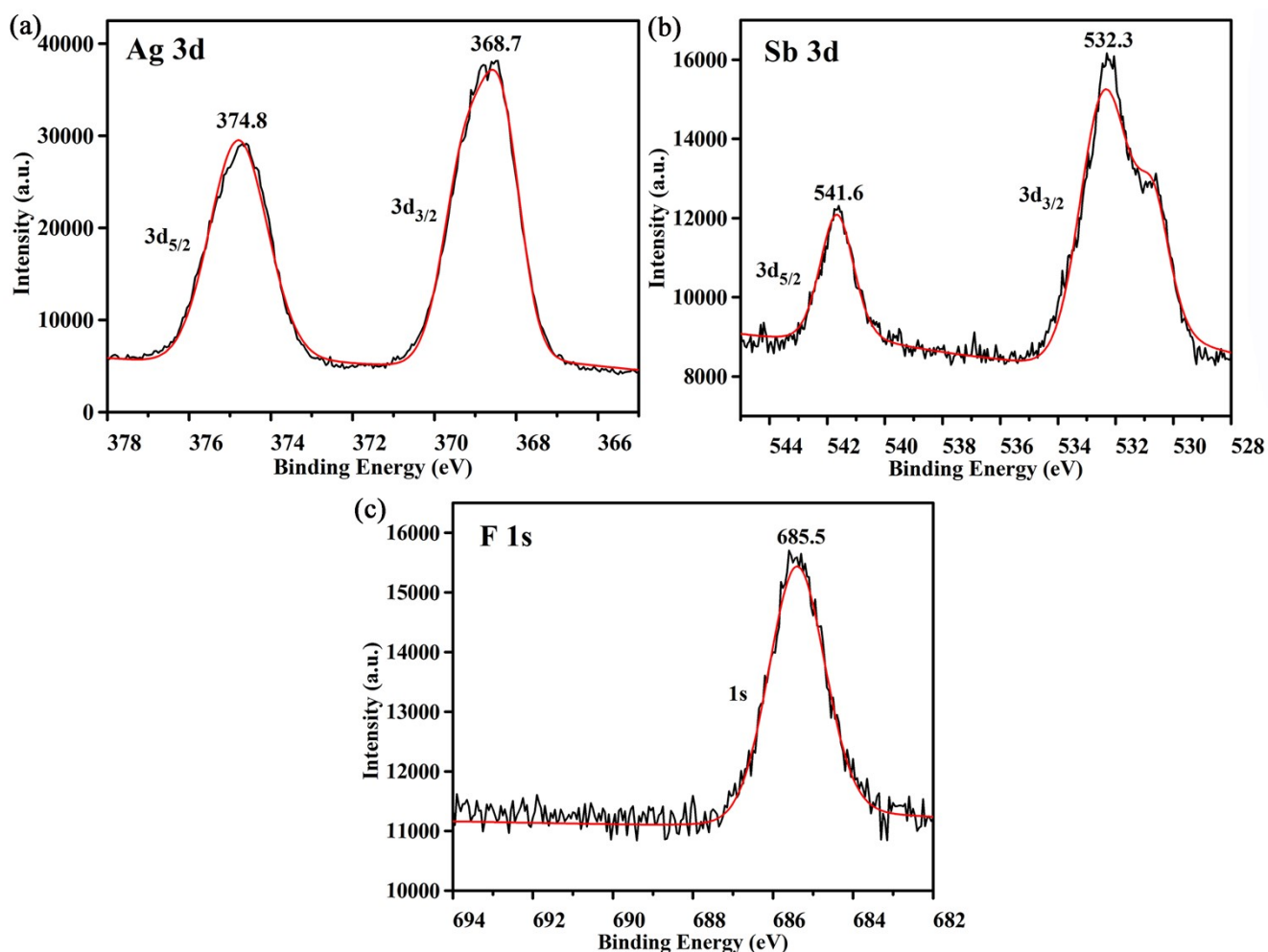


Fig. S3 (a) XPS peak of Ag 3d in Ag_9 . (b) XPS peak of Sb 3d in Ag_9 . (c) XPS peak of F 1s in Ag_9 .

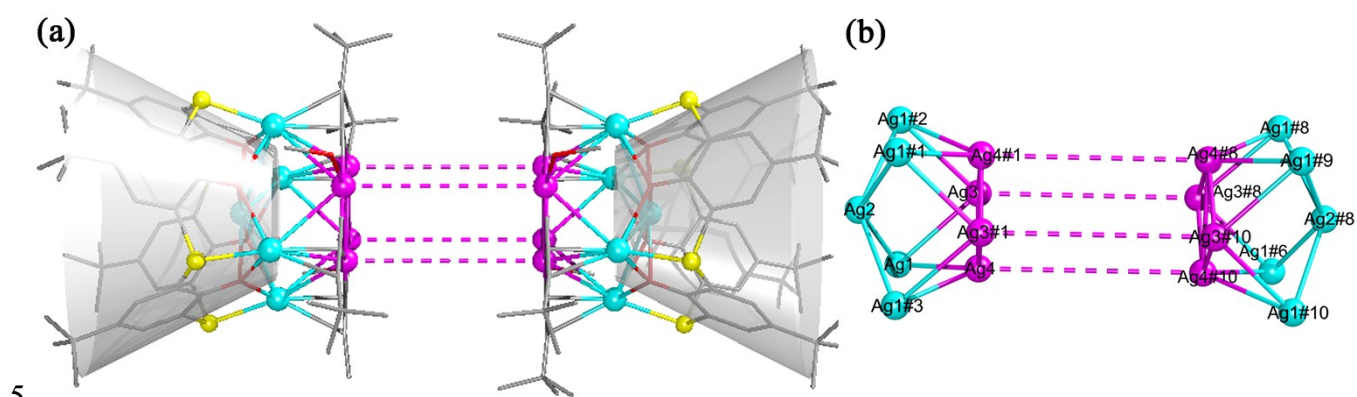


Fig. S4 (a) Side view of two $[\text{Ag}_9(\text{TC4A})(t\text{BuC}\equiv\text{C})_4(\text{CH}_3\text{OH})_2]^+$ cationic cluster in Ag_9 and the grey cone representation of the TC4A^+ ligand, and the $\text{Ag}\cdots\text{Ag}$ distances between the two Ag_9 cores drawn in dotted lines. (b) The two Ag_9 cores in Ag_9 , and the $\text{Ag}\cdots\text{Ag}$ distances between the two Ag_9 cores drawn in dotted lines. Color code: Ag, turquoise, pink; O, red; S, yellow; C, gray-50%.

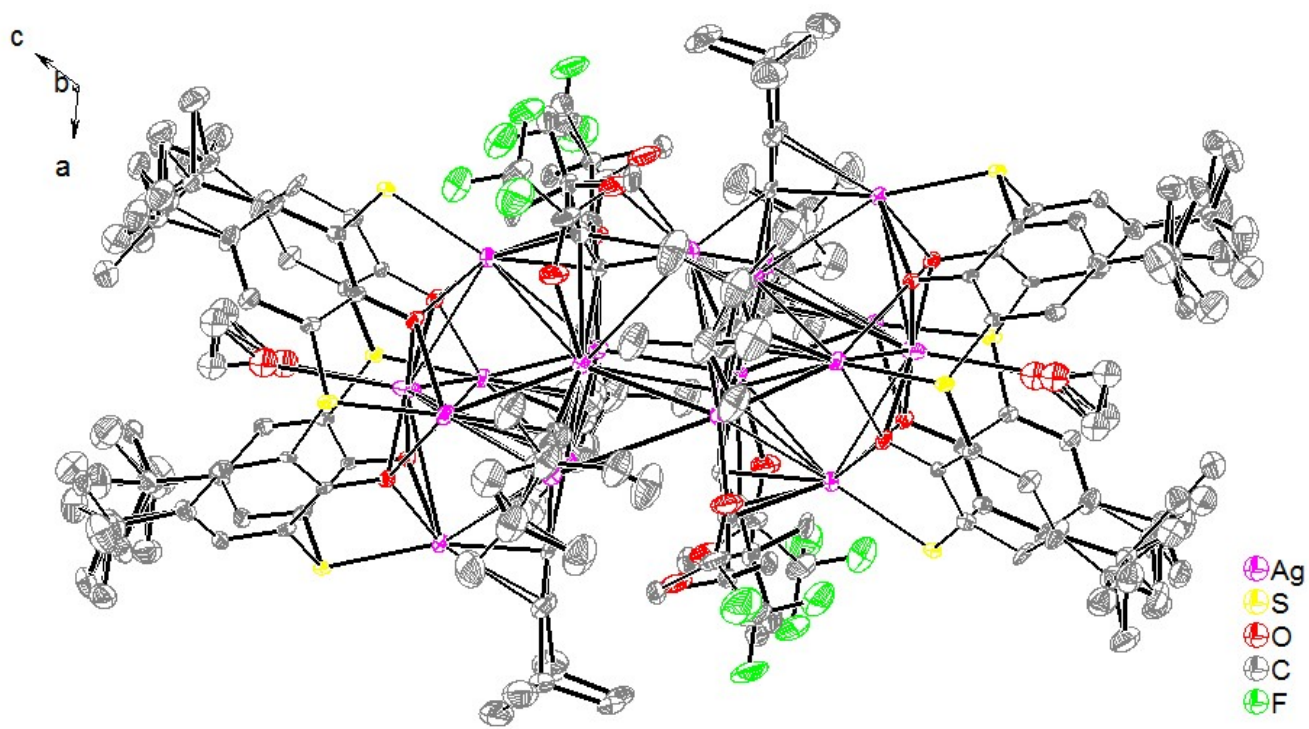


Fig. S5 30% Ellipsoid representations of Ag_{18} containing all disordered atoms. All the hydrogen atoms have been omitted.

5

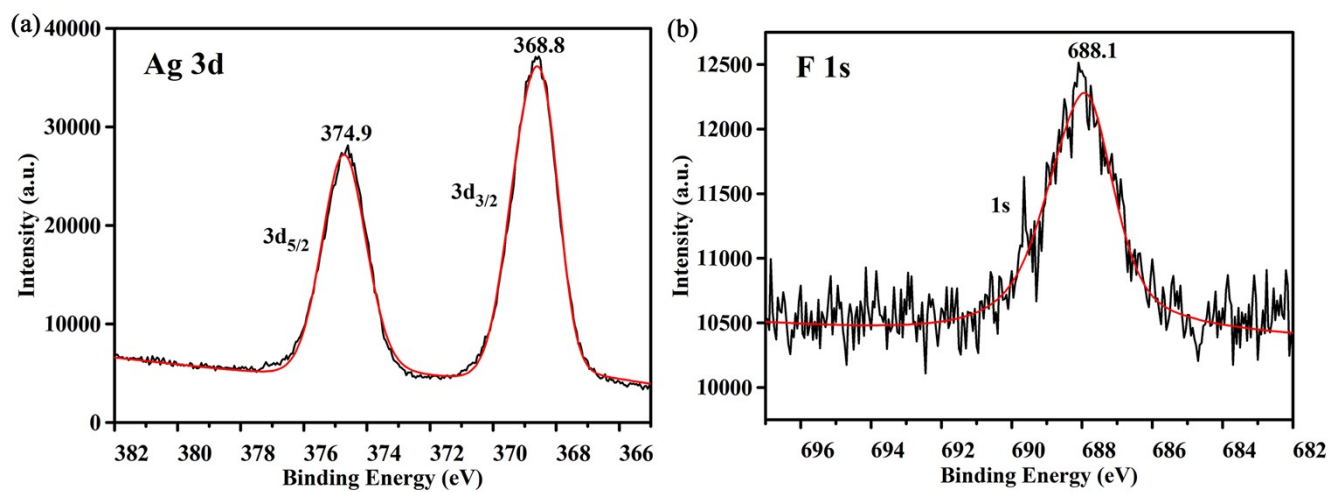


Fig. S6 (a) XPS peak of Ag 3d in Ag_{18} . (b) XPS peak of F 1s in Ag_{18} .

10

^1H NMR

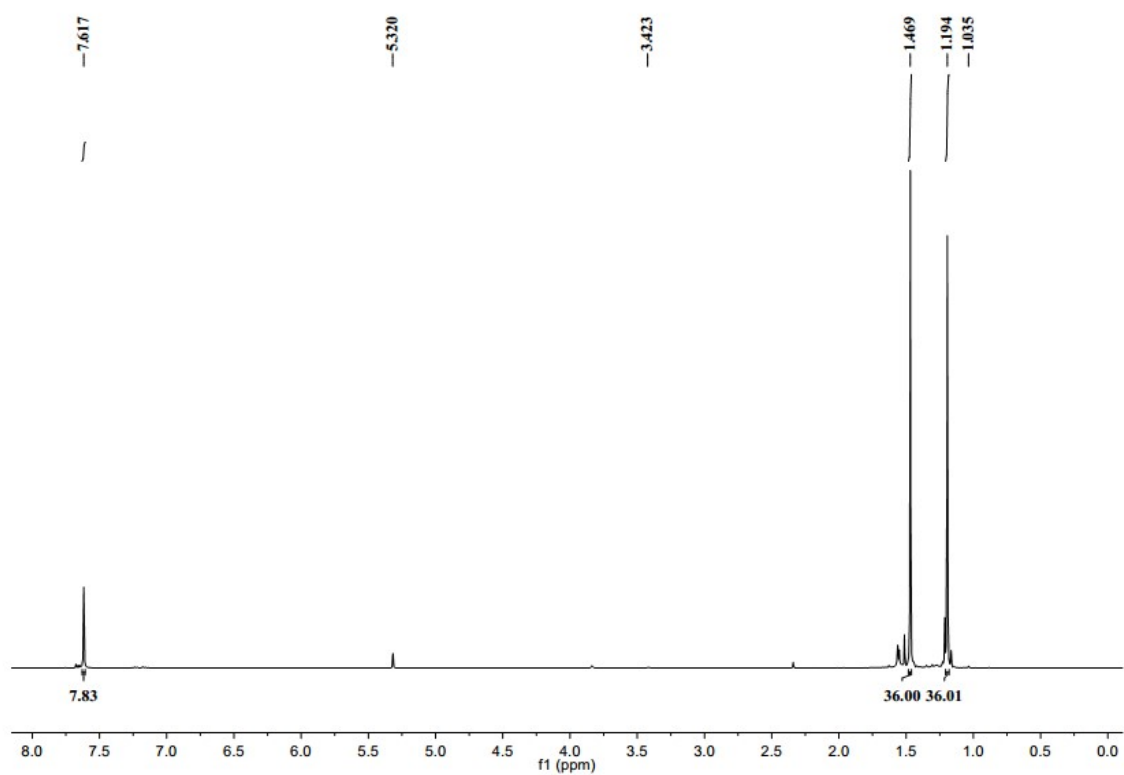


Fig. S7 ^1H NMR of Ag_9 .

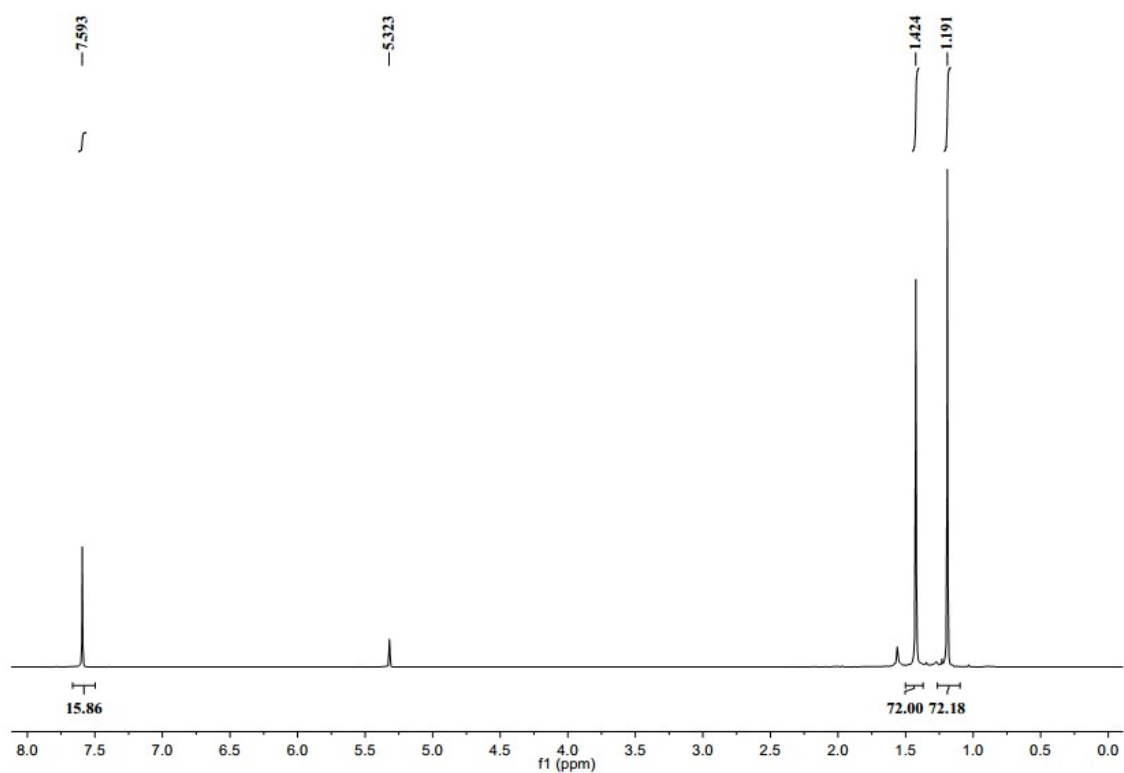


Fig. S8 ^1H NMR of Ag_{18} .

S10

MALDI-TOF mass spectrometry

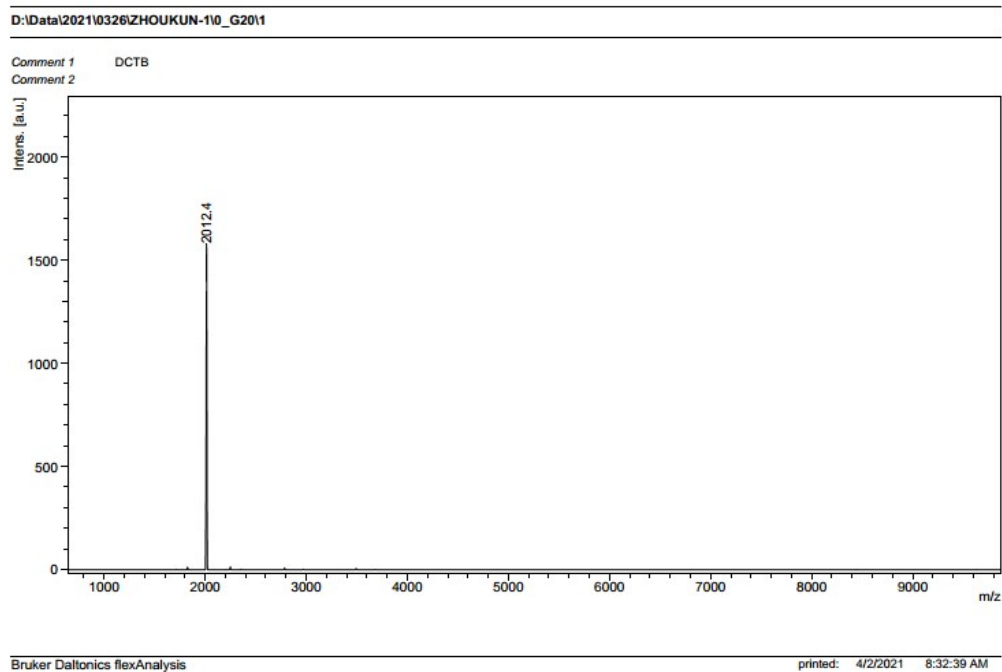
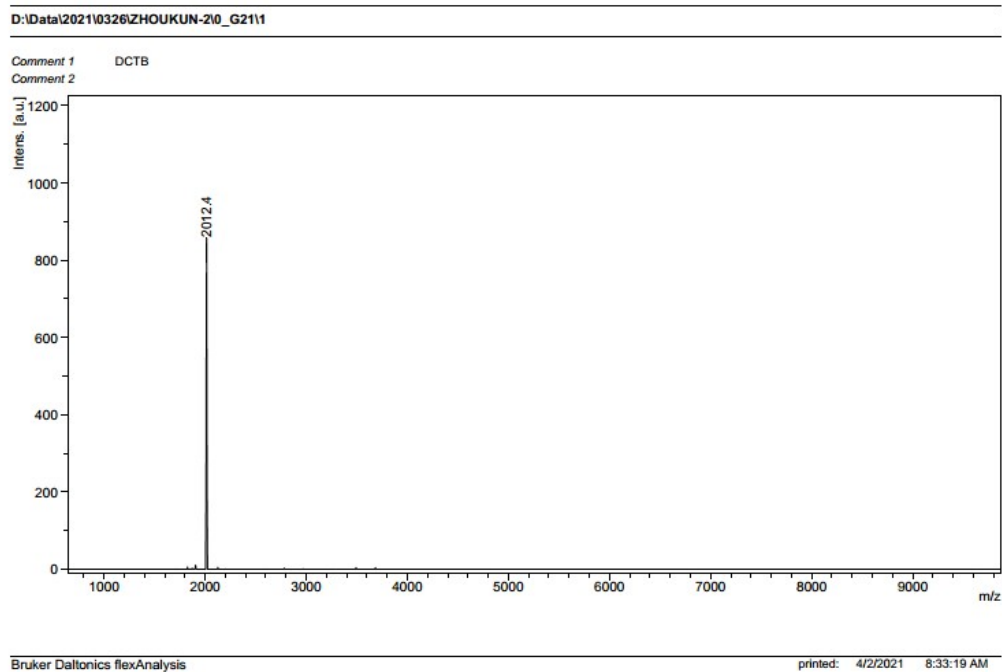


Fig. S9 The full range file of MALDI-TOF MS of the $[\text{Ag}_9(\text{TC4A})(t\text{BuC}\equiv\text{C})_4]^+$ cluster in **Ag₉**.



5 Fig. S10 The full range file of MALDI-TOF MS of the $[\text{Ag}_9(\text{TC4A})(t\text{BuC}\equiv\text{C})_4]^{2+}$ cluster in **Ag₁₈**.

PXRD Measurements

The experimental powder X-ray diffraction patterns of the two compounds are in accordance with the simulated ones from the single crystal X-ray data, confirming the phase purity of the samples.

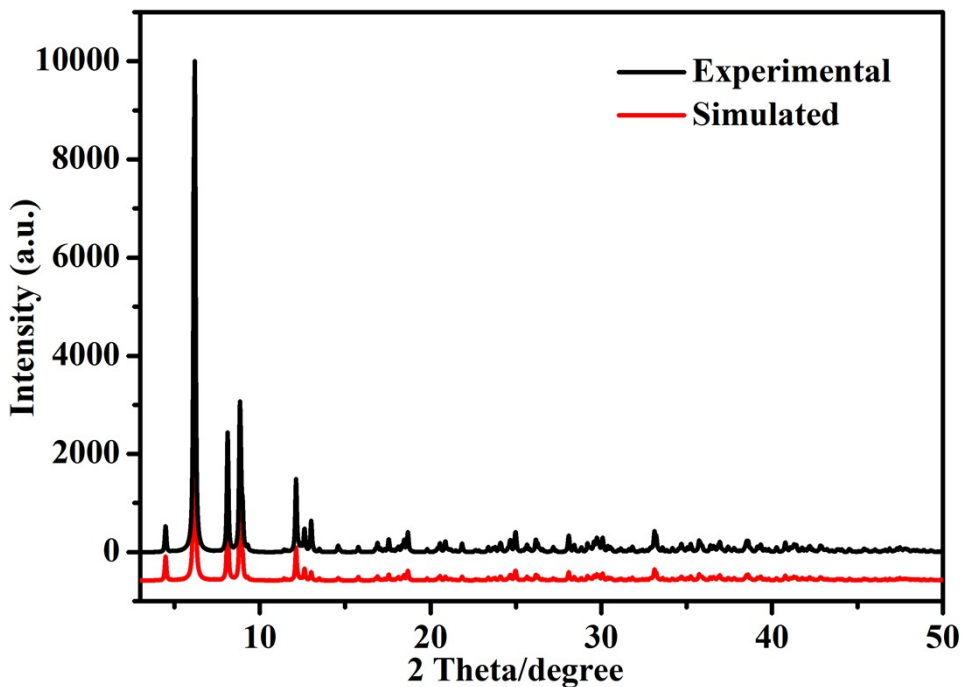


Fig. S11 PXRD of Ag₉.

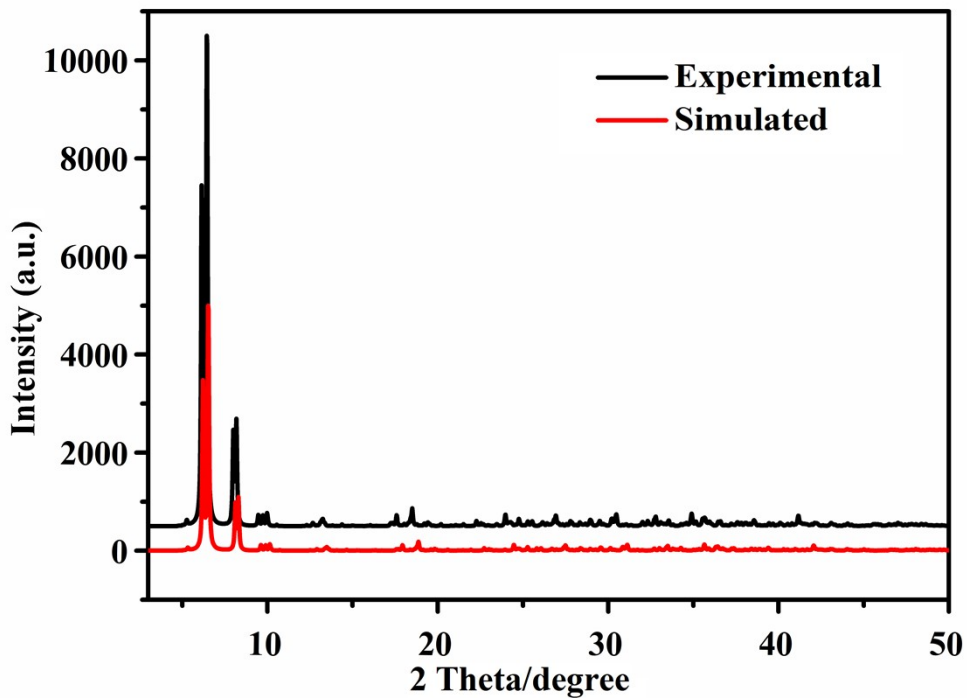


Fig. S12 PXRD of Ag₁₈.

FT-IR Spectra

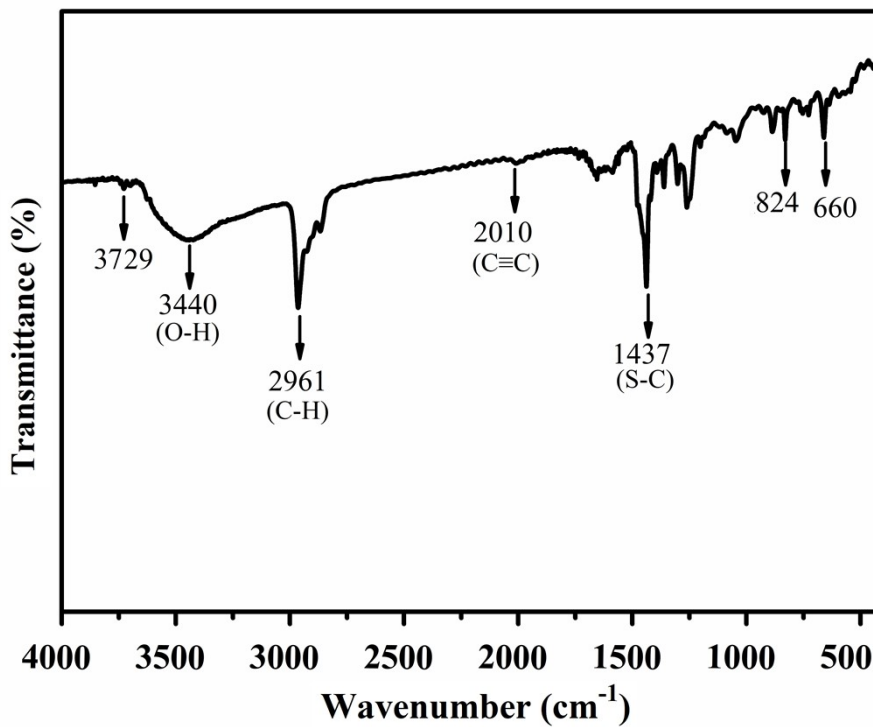


Fig. S13 FT-IR spectrum of Ag₉.

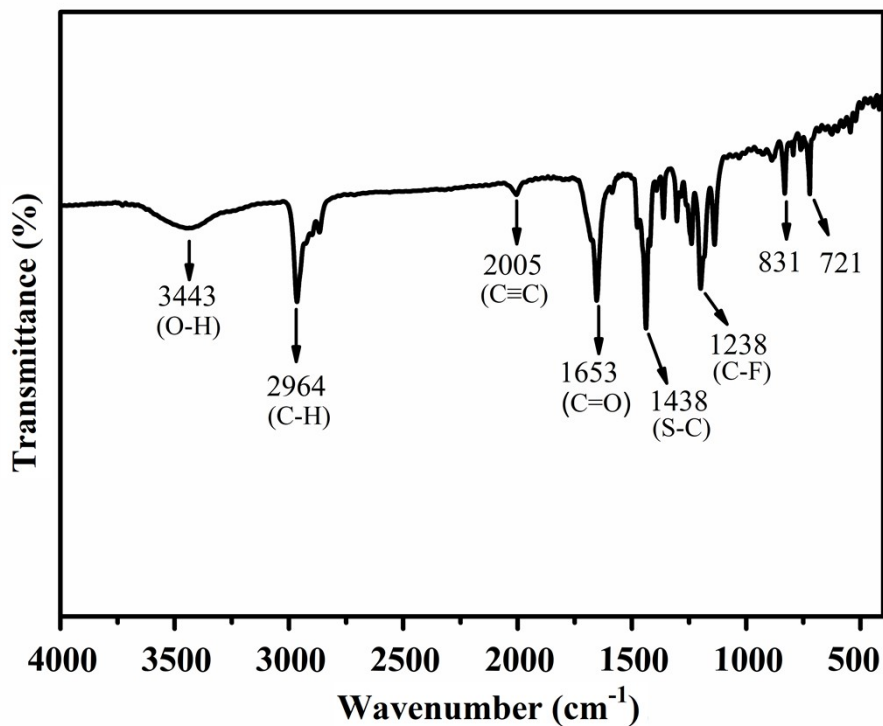


Fig. S14 FT-IR spectrum of Ag₁₈.

TG-DSC Analyses

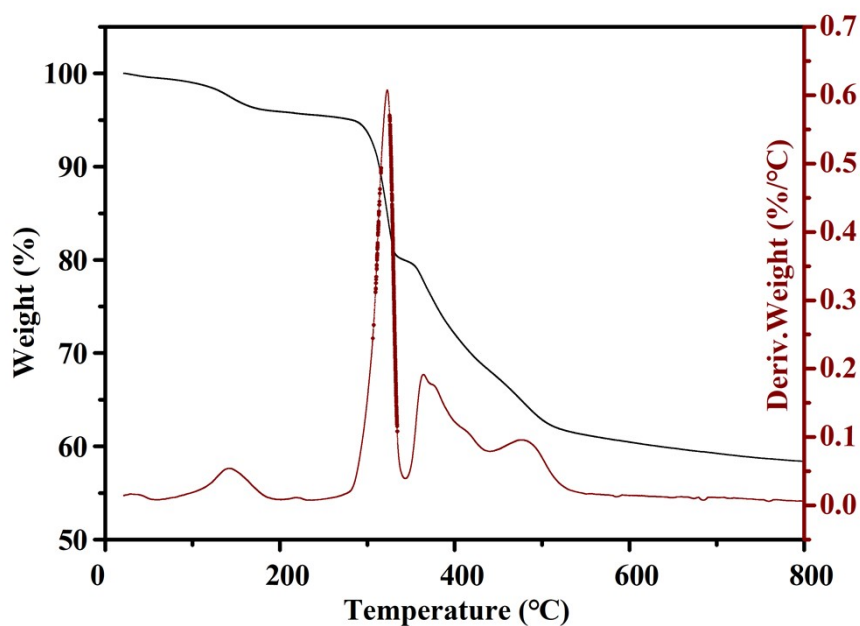


Fig. S15 TG curves of Ag_9 .

As shown in Fig. S16, the weight loss of Ag_{18} from room temperature to 220 °C could be attributed to the loss of CH_3OH molecules attached to the crystal surface. From 220 °C to 290 °C, there is a sharp drop in weight due to the shed of tert-butyl acetylene ligands and CF_3COO^- ligands. After 290 °C, the weight decreased sharply, which can be attributed to the decomposition of thiacalix[4]arene ligands and the collapse of the skeleton of Ag_{18} .

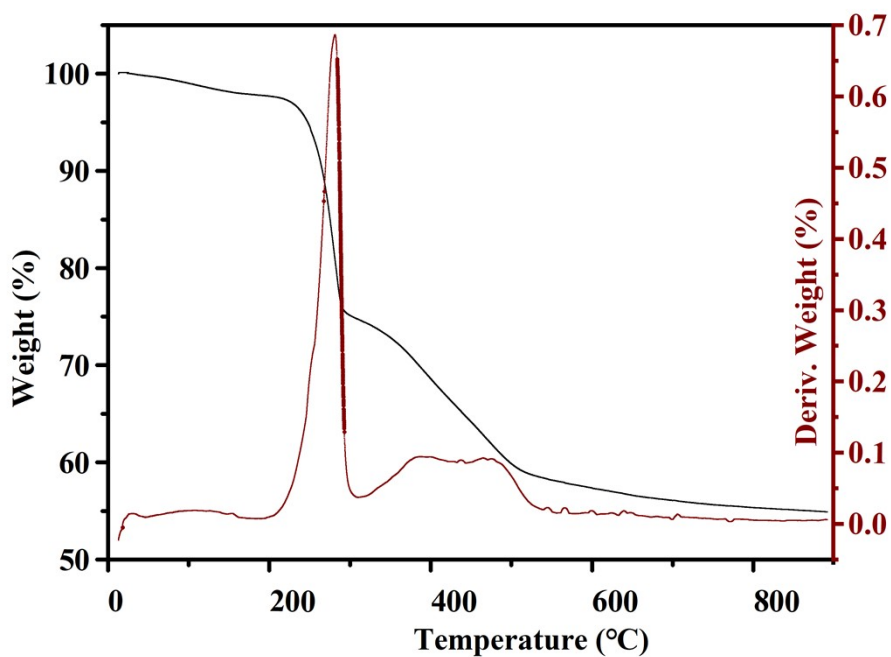


Fig. S16 TG curves of Ag_{18} .

Photocurrent measurement

The photocurrent test was carried out on a CHI660E electrochemistry workstation^{1,2} and in a typical three-electrode system. The crystals (10 mg) of **Ag₉** and **Ag₁₈** were dispersed in 1 mL trichloromethane, the mixture was sonicated for about 30 min. Then a 20 μ L solution was transferred by pipetting gun dropped on the cleaned FTO glass, which apply three to five times in the same way after evaporation under ambient atmosphere. Then a conductive layer of $0.8 \times 1 \text{ cm}^2$ compounds made of AB glue were transferred into a drying oven and kept at 80 °C for 10 h. The coated film was obtained. The prepared FTO glass film was used as working electrode, platinum wire as the counter electrode, Ag/AgCl as the reference electrode and keeping the bias voltage at 10 0.6 V, and a 0.2 M Na₂SO₄ aqueous solution was used as the electrolyte.

Reference:

1. Z. Wang, H.-F. Su, Y.-W. Gong, Q.-P. Qu, Y.-F. Bi, C.-H. Tung, D. Sun and L.-S. Zheng, *Nat. Commun.*, 2020, **11**, 308.
2. P.-P. Zhang, J. Peng, H.-J. Pang, J.-Q. Sha, M. Zhu, D.-D. Wang and M.-G. Liu, *CrystEngComm*, 2011, **13**, 3832–3841.